Clustering of α-Synuclein on Supported Lipid Bilayers: Role of Anionic Lipid, Protein, and Divalent Ion Concentration

Anjan P. Pandey,[†] Farzin Haque,[†] Jean-Christophe Rochet,[‡*] and Jennifer S. Hovis[†*]
[†]Department of Chemistry and [‡]Department of Medicinal Chemistry and Molecular Pharmacology, Purdue University, West Lafayette, Indiana

ABSTRACT α-Synuclein is the major component of Lewy body inclusions found in the brains of patients with Parkinson's disease. Several studies indicate that α-synuclein binds to negatively charged phospholipid bilayers. We examined the binding of α-synuclein to membranes containing different amounts of negatively charged lipids using supported lipid bilayers, epifluorescence microscopy, fluorescence recovery after photobleaching, and bulk fluorescence techniques. The membranes contained phosphatidylcholine and phosphatidylglycerol. In the absence of protein, these lipids mix uniformly. Our results show that the propensity of α-synuclein to cluster on the membrane increases as the concentration of anionic lipid and/or protein increases. Regions on the lipid bilayer where α-synuclein is clustered are enriched in phosphatidylglycerol. We also observe divalent metal ions stimulate protein cluster formation, primarily by promoting lipid demixing. The importance of protein structure, lipid demixing, and divalent ions, as well as the physiological implications, will be discussed. Because membrane-bound α-synuclein assemblies may play a role in neurotoxicity, it is of interest to determine how membranes can be used to tune the propensity of α-synuclein to aggregate.

INTRODUCTION

α-Synuclein has received considerable attention recently because of its connection to Parkinson's disease (PD). A neuropathological hallmark of PD is the presence of cytosolic inclusions named Lewy bodies (1–3) in some of the surviving neurons; these Lewy bodies consist largely of fibrillar α-synuclein (4–7). Three α-synuclein mutants—A53T (8), A30P (9), and E46K (10)—are associated with familial PD, a rare, early-onset form of the disease inherited in an autosomal dominant manner. All three mutants have a greater tendency to self-associate than wild-type α-synuclein (11–16). All of these observations have led to the hypothesis that the aggregation of α-synuclein plays a role in the pathogenesis of PD (reviewed in Dev et al. (17)).

α-Synuclein is thought to be involved in regulating the size of synaptic vesicle pools (18,19) and the release of dopamine (20). The protein contains 140 residues and is ''natively unfolded'' in solution (21). It binds to phospholipid membranes through the N-terminal region; upon binding it adopts an α-helical structure that sits on top of the membrane (22), whereas the C-terminal region remains unstructured (23). The N-terminal region (residues 1–95) consists of seven degenerate, 11-residue repeats, six of which contain a highly conserved motif: ''KTK(E/Q)GV'' (22,24). This is consistent with an amphipathic helical domain with the polar face having a net positive charge (23,25–27). Unsurprisingly, the binding of α-synuclein is enhanced when anionic lipids are present (22,28,29). Whether the conversion of α-synuclein to β-sheet structures is promoted (30–32) or inhibited (32–34) upon binding to membranes is at present an open question. It is clear that α-synuclein avidly interacts with lipids; however, further studies of this interaction are needed to understand both the native function of α-synuclein and the mechanism by which it becomes toxic.

In this study, supported lipid bilayers and epifluorescence microscopy were used to examine the interaction of α-synuclein with membranes. Supported lipid bilayers can be formed on appropriately treated solid supports by either vesicle fusion or Langmuir-Blodgett/Langmuir-Schaffer transfer (35). In either method, a thin water layer is trapped between the bilayer and the support, allowing the lipids to retain their natural fluidity (36). By labeling the lipids and the protein, it is possible to monitor the spatial distribution of both macromolecules simultaneously. In the experiments shown herein, the lipid bilayer was composed of phosphatidylglycerol (PG) and phosphatidylcholine (PC) in varying ratios. These lipids were chosen because they give an anionic/zwitterionic combination wherein the lipids mix nearly ideally in the absence of protein or divalent ions (37,38). Herein we examine the effect of anionic lipid concentration, protein concentration, and divalent ion concentration on the formation of protein clusters. The biophysics and physiological implications of the results are discussed.

MATERIALS AND METHODS

Stock solutions of L-α-phosphatidylcholine (egg PC), L-α-phosphatidylglycerol (egg PG), and 1-palmitoyl-2-[6-[(7-nitro-2-1,3-benzoxadiazol-4-yl) amino]hexanoyl]-*sn*-glycero-3-phosphocholine (NBD-PC) in chloroform were purchased from Avanti Polar Lipids (Birmingham, AL) and used without further purification. Ethylenediaminetetra-acetic acid (EDTA) was purchased from Sigma Chemical (St. Louis, MO). Sodium chloride (NaCl), sodium hydroxide (NaOH), and 4-(2-hydroxyethyl)-1-piperazineethanessulfonic acid (HEPES, free acid) were purchased from Mallinckrodt Chemicals

Submitted August 12, 2008, and accepted for publication October 9, 2008.

*Correspondence: rochet@pharmacy.purdue.edu or jennifer.hovis@gmail.com

Editor: William C. Wimley.

0006-3495/09/01/0540/12 $2.00

doi: 10.1016/j.bpj.2008.10.011

(Philipsburg, NJ). Alexa Fluor 647 carboxylic acid, succinimidyl ester was purchased from Invitrogen (Carlsbad, CA). The Superdex 200 gel-filtration column was purchased from GE Healthcare Life Sciences (Piscataway, NJ), and the Microcon YM-100 centrifugal filter units were obtained from Millipore (Bedford, MA).

Vesicle and supported lipid bilayer preparation

Lipid stock solutions in chloroform were mixed in the appropriate molar ratios, dried under a stream of nitrogen, and placed under vacuum for 1 h. After drying, 30, 40, and 50 mol % PG lipid films were rehydrated in 100 mM NaCl solution, and 0% PG was rehydrated in 50 mM HEPES, 0.1 mM EDTA, and 100 mM NaCl buffer, pH 7.4. Large unilamellar vesicles were prepared by extruding the solution 21 times through 100 nm polycarbonate membranes. The vesicle solution was then centrifuged for 5 min at 14,000 rpm (Eppendorf Minispin Plus). The vesicles were stored at room temperature and shielded from light. Supported lipid bilayers were formed by vesicle fusion inside a 60 μL perfusion chamber (Molecular Probes, Eugene, OR) on appropriately treated glass slides. PG vesicles (30, 40, and 50 mol %) were mixed with 750 mM NaCl solution at a 1:1 ratio before fusion. After 15 min, excess vesicles were removed from the perfusion chamber using 750 mM NaCl solution; the pH was adjusted using 50 mM HEPES, 0.1 mM EDTA, and 750 mM NaCl, pH 7.4 buffer; and the slide was finally rinsed with 50 mM HEPES, 0.1 mM EDTA, pH 7.4 buffer to remove salt. Before fusion, 0 mol % PG vesicles were mixed with 50 mM HEPES, 0.1 mM EDTA, pH 7.4 buffer at a 1:1 ratio, and the excess vesicles were removed with the same buffer. Before bilayer formation, glass coverslips were washed in ICN 7X detergent (VWR International, Chicago, IL), rinsed profusely in deionized water, dried with a stream of nitrogen, and baked at 450°C for 4 h. The slides and vesicles were used within a day of preparation. At least 3 mL of buffer were passed through the perfusion chamber to ensure complete exchange. The bilayers were kept hydrated in 50 mM HEPES, 0.1 mM EDTA, pH 7.4 buffer before protein addition. Apart from using buffers with no EDTA, all other conditions were kept the same in the experiments involving calcium.

Expression, purification, and labeling of α-synuclein

Human wild-type α-synuclein was expressed in *Escherichia coli* and purified as described previously (12). The protein was preferentially labeled at the N-terminus: monomeric α-synuclein (0.56 mM in 225 μL PBS, pH 7.0) was mixed with Alexa Fluor 647 carboxylic acid, succinimidyl ester (0.25 mg in 25 μL dimethyl sulfoxide (DMSO)). The mixture was placed on a Microplate shaker at 800 rpm for 2 h. The protein solution was then loaded onto a Superdex 200 gel-filtration column and eluted in 20 mM HEPES, pH 7.4. The protein concentration and degree of labeling were determined using ultraviolet-visible absorbance measurements (the degree of labeling of the protein was typically 20%, mol/mol). The protein was then aliquoted and stored at −20°C. Before each experiment, an aliquot was thawed and centrifuged through a Microcon YM-100 centrifugal filter unit with a molecular-weight cutoff of 100 kDa to remove any aggregates.

Calculating the amount of α-synuclein adsorbed

A Nikon TE2000 fluorescence microscope equipped with a 40× oil immersion objective, an Alexa filter set (Chroma Technology, Rockingham, VT) and a silicon avalanche photodiode (APD) single photon counting module (SPCM-AQR-16-FC, PerkinElmer, Vaudreuil, Quebec, Canada) was used to focus, collect, and count the emitted fluorescence. An arc lamp was used to monitor the protein and a LabVIEW program was used to acquire the counts from the APD. To minimize photobleaching of the fluorophore during the counting period, the lamp intensity was reduced using a 5X (focal transmission of 1×10^5) neutral density filter (NE50B; Thorlabs, Newton, NJ). α-Synuclein (2.6 μM, 60 μL) was added to phospholipid bilayers and incubated for 15 min. Protein counts were obtained before and after the unbound protein was rinsed off with 2.5 mL of 50 mM HEPES, 0.1 mM EDTA, pH 7.4 buffer.

Imaging of supported lipid bilayers and protein

A Nikon (Tokyo, Japan) TE2000 fluorescence microscope equipped with a Cascade 512B CCD camera (Roper Scientific, Tucson, AZ) was used. An X-Cite 120 arc lamp (EXFO) was used as a light source. For imaging, 0.25 mol % tail-labeled NBD-PC was present in the bilayer and the protein was labeled with Alexa Fluor 647. The NBD and Alexa fluorophores were imaged using NBD and Alexa 647 filter sets, respectively (Chroma Technology). Images were acquired using a 100×, 1.30 NA objective. The images were contrasted in each case to make any features appear clearly. For quantitative comparisons, linescans are also provided. From all the linescans, appropriate backgrounds (dark noise of the camera, glass autofluorescence, etc.) were subtracted off using counts obtained from a bilayer without the NBD fluorophore.

Fluorescence recovery after photobleaching

The fluorescence recovery after photobleaching (FRAP) measurement system is discussed in detail elsewhere (39). Briefly, a Nikon TE2000 fluorescence microscope equipped with a 40× oil immersion objective, an NBD filter set (Chroma Technology) and an APD single photon counting module (SPCM-AQR-16-FC, PerkinElmer, Vaudreuil, Canada) was used to focus, collect, and count the emitted fluorescence. A 15 mW Argon ion laser (488 nm Melles Griot) was used to both bleach and monitor the lipid bilayer. To reduce further photobleaching of the fluorophore during the recovery period, the laser intensity was reduced 100,000-fold using a 5X (focal transmission of 1×10^5) neutral density filter (NE50B, Thorlabs, Newton, NJ). A LabVIEW program was used to acquire the counts from the APD, control the filter wheel, and trigger the shutter (Uniblitz; VA, Rochester, NY).

RESULTS

Some reports in the literature suggest that membranes promote α-synuclein aggregation (30–32), whereas others suggest that membranes inhibit α-synuclein aggregation (32–34). Herein we describe three control parameters that can be used to adjust the propensity of α-synuclein to adopt an aggregate-like appearance: anionic lipid concentration, protein concentration, and divalent ion concentration.

Supported lipid bilayers prepared by vesicle fusion were used as a model membrane system. The bilayers were imaged using epifluorescence microscopy, and the fluidity of each bilayer was checked with FRAP. The bilayers were composed of varying amounts of egg PG and egg PC. Egg PG is prepared from egg PC by the action of phospholipase D; therefore, the tail compositions were identical for the phospholipids used in this study. After varying concentrations of α-synuclein (in 50 mM HEPES, 0.1 mM EDTA, pH 7.4) were added to the bulk solution, the bilayer was incubated for 15 min. Unbound protein was then rinsed off with buffer, and images of the protein and lipid were acquired. The bilayers contained 0.25 mol % NBD-PC, and ~20% of the protein was labeled with Alexa 647. The excitation and emission spectra of the fluorophores are far enough apart that fluorescence resonance energy transfer is not a concern.

Anionic lipid

Supported lipid bilayers with 0, 30, 40, and 50 mol % PG were used to examine the effect of anionic lipids on protein binding. Fig. 1 shows images acquired after the bilayers were exposed to 2.6 μM α-synuclein (1:1 protein/lipid ratio, mol/mol). The protein bound relatively uniformly or with a small degree of clustering to bilayers containing 0 mol % PG or 30 mol % PG, respectively (Fig. 1, *e* and *f*; *dotted line* in linescans *i* and *j*). The images are individually contrasted such that any features are emphasized; for quantitative comparisons, see the linescans (from which appropriate backgrounds have been subtracted). Also, the lipid bilayers remained uniform for the 0 and 30 mol % PG bilayers (Fig. 1, *a* and *b*; *solid line* in linescans *i* and *j*), as they were before protein addition (not shown). The integrated protein intensity counts for the 0 and 30 mol % PG bilayers were within the error limit (Fig. 2), suggesting that similar amounts of the protein were adsorbed onto the bilayer under these conditions. To determine the amount of protein that corresponds to average protein intensities for the 0 and 30 mol % PG, protein counts for the 0 mol % PG were monitored before and after rinsing excess unbound protein (see Materials and Methods for details). The amount of bound protein was >7%. This number is an overestimate of the amount of adsorbed protein because the focal volume will not be able to sample the entire bulk solution due to the limitation imposed by the objective working distance. We note that when 2% of the protein is bound to the bilayer, there is one protein for every 50 lipids,

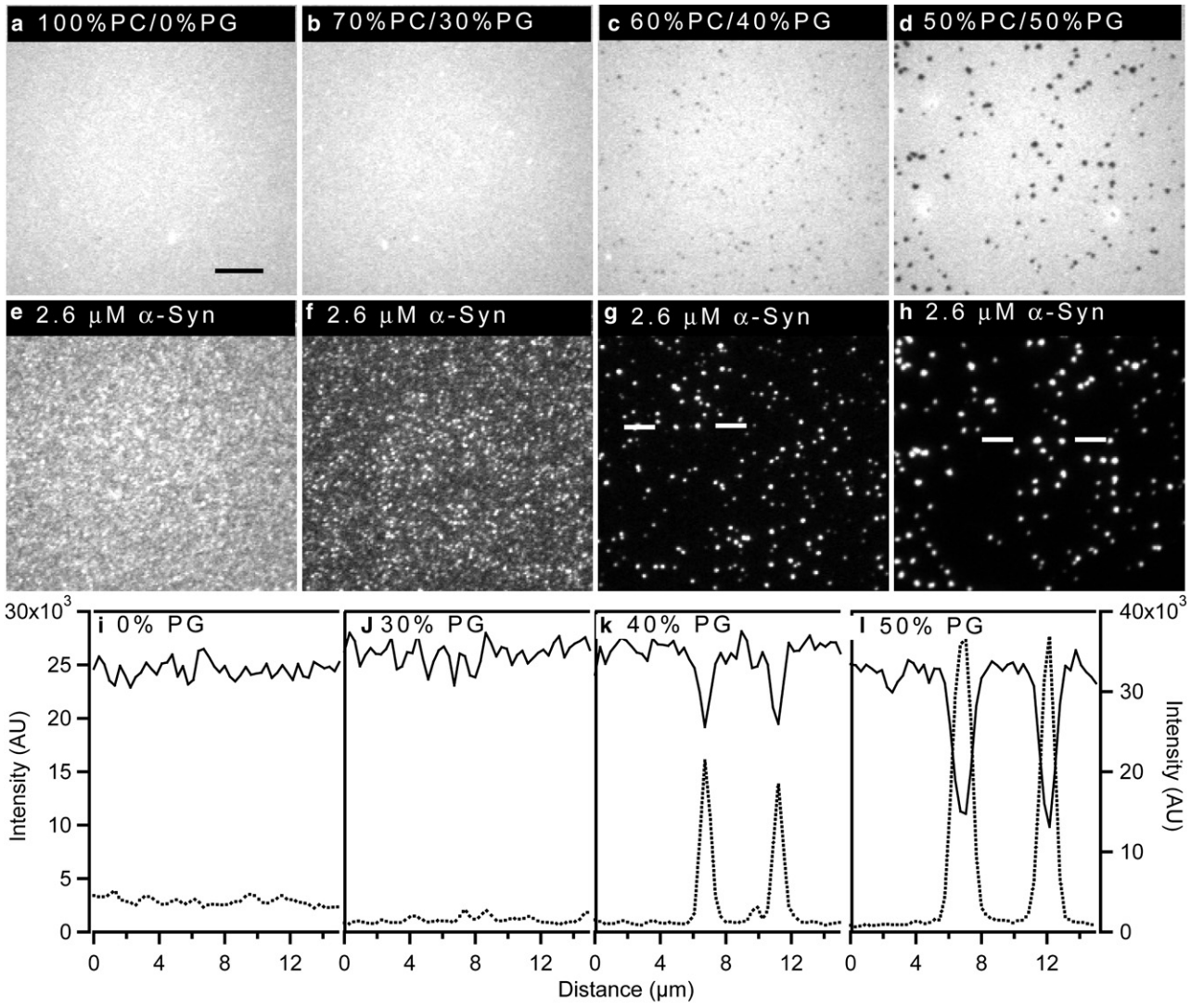

FIGURE 1 Ability of α-synuclein to form clusters on a supported bilayer increases with increasing anionic phospholipid content. Excess α-synuclein was removed before imaging. Epifluorescence images of PC/PG bilayers after the addition of 2.6 μM α-synuclein (bilayers: *a–d*, protein: *e–h*). The bilayers contained 0.25 mol % NBD-PC and the protein was labeled with Alexa Fluor 647. (*i–l*) Lipid linescans (*solid line*, scale on left *y* axis) and protein linescans (*dotted lines*, scale on right *y* axis) for different mol % PG as indicated on the plots. Linescans for 40 and 50 mol % PG were obtained from regions between white lines in images *g* and *h*, respectively. A 100×, 1.3 NA objective was used to acquire the images. The scale bar represents 10 μm.

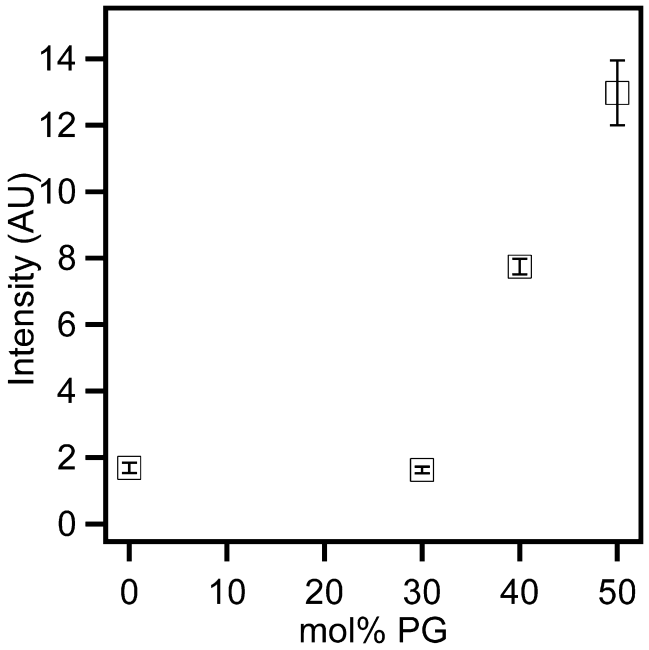

FIGURE 2 Average intensity of α-synuclein on supported bilayers composed of varying amounts of PG. The bilayers were incubated with 2.6 μM α-synuclein. Each data point represents the average of 12 images. The error bar represents the standard deviation of the mean.

and this amount corresponds roughly to a monolayer of protein coverage. Thus, there could be a maximum of ~3 monolayers of protein coverage at 0 and 30 mol % PG.

In contrast, large-scale clustering of the protein was observed on bilayers containing 40 and 50 mol % PG (Fig. 1, *g* and *h*; *dotted line* in linescans *k* and *l*). For the linescans, protein clusters that correlate to visible darker regions in the lipid bilayer were chosen; the intensities of all the clusters that encompass several pixels are very similar. Small and less bright clusters were avoided because small clusters below the size of a single pixel will appear less intense than they actually are. When more than 30 mol % of anionic PG was incorporated, the amount of α-synuclein bound on the supported lipid bilayers increased as a function of negatively charged lipid (Fig. 2). Furthermore, increasing the amount of PG from 40 to 50 mol % resulted in protein clusters that were ~2 times higher in intensity (Fig. 1, *dashed line*, linescans *k* and *l*). In addition, lipid phase separation was visible at 40 and 50 mol % PG (Fig. 1, *c* and *d*; *solid line* in linescans *k* and *l*). The images are contrasted to clearly show the light and dark regions (the actual differences in intensity between the light and dark regions in Fig. 1, *c* and *d*, are ~30 and ~50%, respectively). The fluorescent NBD moiety is attached to the tail of a PC lipid. This suggests that dark lipid domains in Fig. 1, *c* and *d*, are enriched in negatively charged PG lipids. The lipids are held close to the surface via hydration, electrostatic, steric, and van der Waals forces, and due to strong coupling between the bilayer and the glass substrate. As a consequence, domains are usually restrained from coalescing (36). The fact that the domains are micrometers in diameter, coupled with the differential partitioning of the NBD-PC, indicates that phase separation has occurred. To determine whether the lipids in both regions are mobile, FRAP experiments were performed. Rapid, essentially complete (>95%) recovery of both the bright and dark regions was observed, indicating that both regions are fluid. It was previously suggested that α-synuclein binding results in the reorganization of the lipids (40); to our knowledge, the data presented here are the first direct experimental observation of such reorganization. The data also confirm that α-synuclein clustering requires the presence of anionic phospholipids on the bilayer surface, and its binding increases with increasing amounts of negatively charged lipids.

Protein concentration

Data from previous studies suggest that α-synuclein aggregation is promoted by the binding of the protein to phospholipid membranes, especially at a high protein/lipid ratio (30,34). We hypothesized that the α-synuclein clusters observed on supported bilayers enriched with anionic phospholipid might be similar to the membrane-bound α-synuclein aggregates described earlier, and that these aggregates should form more readily upon increasing the protein concentration. To address this hypothesis, we examined the effect of the concentration of α-synuclein on clustering of the protein at the membrane surface. Before protein addition, 50 mol % PC/ 50 mol % PG bilayers were uniformly mixed. Depending on the amount of protein added, lipid demixing could be observed. Fig. 3, *a* and *b*, show images of bilayers containing 50 mol % PG after the addition of 0.26 and 2.6 μM α-synuclein. Protein binding was relatively uniform at the lower concentration of 0.26 μM, equivalent to a 1:10 protein/lipid ratio, mol/mol (Fig. 3 *c*; *dotted line* in linescan *e*). Although there were a small number of low-intensity clusters under these conditions (Fig. 3 *c*), there was no evidence of lipid phase separation (Fig. 3 *a*). Similarly, 0, 30, and 40 mol % PG bilayers did not undergo phase separation upon the addition of 0.26 μM α-synuclein.

As the concentration of protein was raised from 0.26 to 2.6 μM (the concentration used in Fig. 1), the amount of protein adsorbed onto the bilayer increased. This 10-fold increase in protein concentration led to a large-scale α-synuclein clustering (Fig. 3 *d*; *solid line* in linescan *e*), along with lipid phase separation (Fig. 3 *b*). At an even higher concentration of α-synuclein (5.2 μM; 2:1 protein/lipid ratio, mol/mol), protein binding remained predominantly uniform or weakly clustered on bilayers containing 0 mol % PG or 30 mol % PG, respectively, whereas clustering and lipid phase separation were further enhanced in bilayers containing 40 and 50 mol % PG.

Addition of calcium after α-synuclein

A previous report suggested that calcium interacts with the C-terminal domain of α-synuclein and promotes its interaction

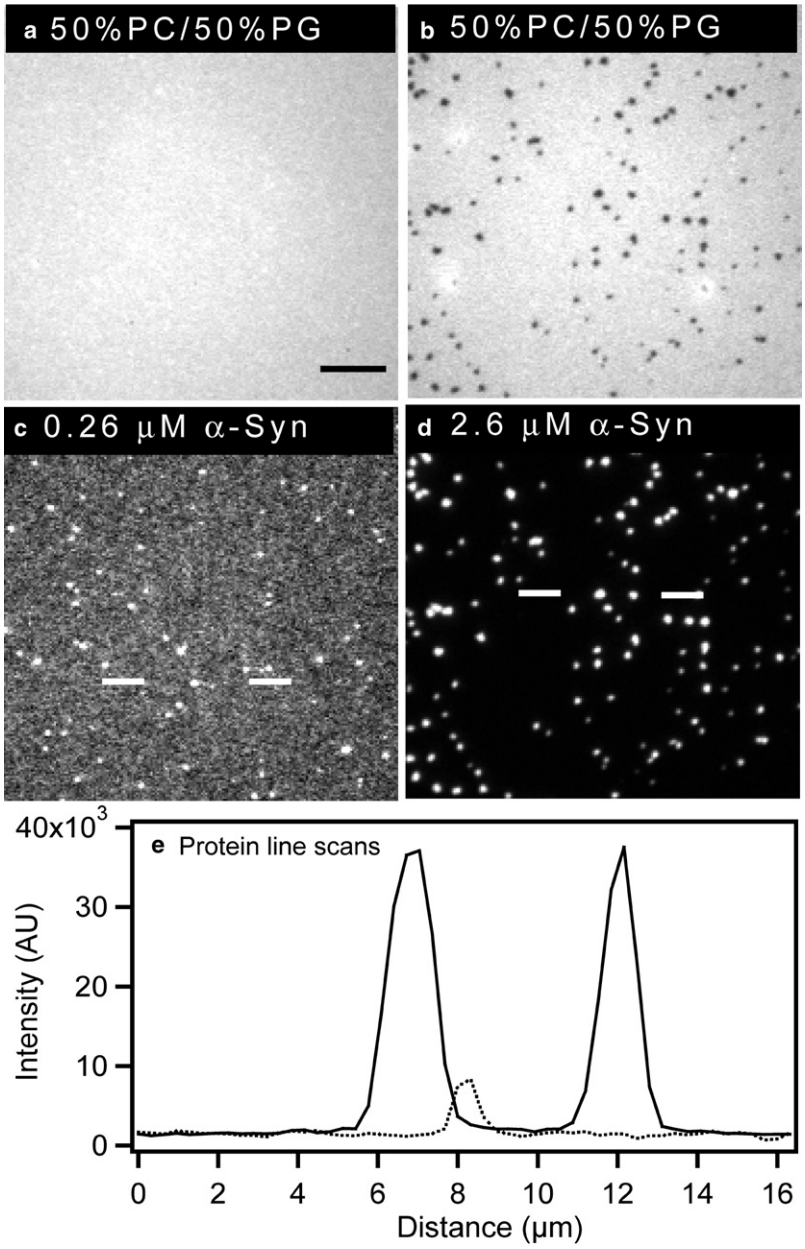

FIGURE 3 Ability of α-synuclein to form clusters on a supported bilayer increases with increasing protein concentration. Before imaging excess α-synuclein was removed. Epifluorescence images of 49.75 mol % PC/ 50 mol % PG/0.25 mol% NBD-PC bilayers after the addition of Alexa Fluor 647-labeled wild-type α-synuclein (bilayers: *a* and *b*; protein: *c* and d). Two different concentrations of α-synuclein were added: 0.26 μM (*a* and *c*) and 2.6 μM (*b* and *d*). (*e*) Protein linescans for 0.26 μM (*dotted line*) and 2.6 μM (*solid line*) α-synuclein were obtained from the regions between white lines indicated in images *c* and *d*. A 100×, 1.3 NA objective was used to acquire the images. The scale bar represents 10 μm.

with a phospholipid bilayer, thereby stimulating the formation of membrane-bound aggregates (41). Accordingly, we hypothesized that the clustering of α-synuclein on a PG-containing bilayer might be enhanced by the addition of calcium. To address this question, we examined whether calcium ions induced α-synuclein clustering on PG-containing membranes under conditions where the protein bound nearly uniformly to the lipid bilayer. A dramatic rearrangement of protein bound to a 50 mol % PG bilayer was observed when calcium was added after the addition of 0.26 μM α-synuclein (Fig. 4). The bilayer was formed as described above, and after a 15-min incubation unbound protein was rinsed away. At low α-synuclein concentration, the protein exhibited limited clustering (Fig. 4 *c*; *dotted line* in linescan *e*). As expected, the bilayer was uniform (Fig. 4 *a*). The bulk solution was then exchanged with 1 mM $CaCl_2$, 50 mM HEPES, pH 7.4 to introduce calcium into the lipid-protein mixture. After calcium addition, bright protein clusters were formed (Fig. 4 *d*; *solid line* in linescan *e*), and corresponding PG-enriched domains were observed in the bilayer (Fig. 4 *b*). The intensity of protein clusters after calcium addition was ~3 times higher than that of the ''weak'' clusters formed in the absence of calcium (compare Fig. 4, *c* and *d*). Additionally, the baseline of the linescan dropped after calcium addition (Fig. 4 *e*), strongly suggesting that the protein on the surface reorganized into the clusters (the CCD camera is sufficiently sensitive that the drop in baseline cannot be due to photobleaching). The lipid and protein images acquired after the addition of 2.6 μM

α-synuclein (Fig. 1, *d* and *h*, or Fig. 3, *b* and *d*) or 0.26 μM α-synuclein plus 1 mM calcium (Fig. 4, *b* and *d*) were strikingly similar except for the fact that the intensity of the clusters was approximately half as great in the second case. This difference was likely due to the fact that less protein was added to the solution.

Similar results were obtained for bilayers containing 30 and 40 mol % PG and calcium concentrations as low as 300 μM. However, calcium did not cluster protein bound to 0 mol % PG bilayers.

Addition of calcium before α-synuclein

In addition to its interaction with α-synuclein, it is well known that calcium binds to and reorganizes lipids (42,43). In particular, the addition of calcium (5 mM) to a 3:1 PC/PG bilayer has been shown to cause lipid phase separation after 12 h (42). Accordingly, we wondered whether the reorganization observed in the experiments outlined above was promoted by lipid-ion-protein interactions or by ion-induced lipid reorganization that then promoted

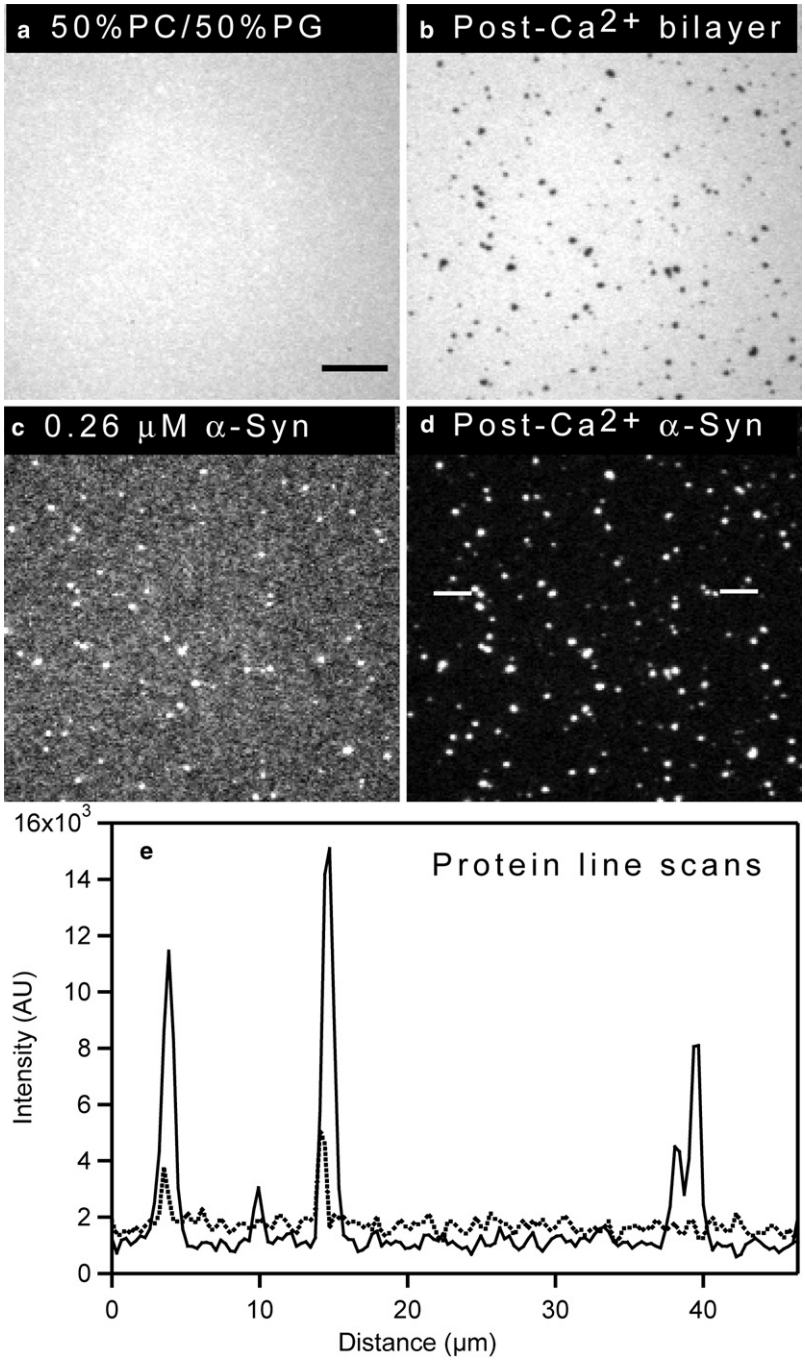

FIGURE 4 α-Synuclein exhibits more pronounced clustering on a supported bilayer in the presence of Ca^{2+} (addition of Ca^{2+} after the protein). Epifluorescence images of a 49.75 mol % PC/ 50 mol % PG/0.25 mol % NBD-PC bilayer and α-synuclein before and after calcium addition are shown. (*a* and *c*) Bilayer (*a*) and protein (*c*) before addition of 1 mM $CaCl_2$, 50 mM HEPES, pH 7.4 buffer. (*b* and *d*) Bilayer (*b*) and protein (*d*) after addition of 1 mM $CaCl_2$, 50 mM HEPES, pH 7.4 buffer. (*e*) Linescan profiles of protein before (*dotted line*) and after (*solid line*) addition of calcium. Excess α-synuclein was removed before imaging. The protein linescan for α-synuclein in the presence of calcium was taken from the region between white lines indicated on *d*. A 100×, 1.3 NA objective was used to acquire the images. The scale bar represents 10 μm.

clustering. To address this question, we examined the effect of adding calcium before α-synuclein.

The addition of calcium before α-synuclein resulted in lipid domains enriched in negatively charged PG lipids. A 30 mol % PG bilayer was formed, and the bulk solution (50 mM HEPES, 0.1 mM EDTA, pH 7.4) was exchanged with 1 mM $CaCl_2$, 50 mM HEPES, pH 7.4 buffer. The bilayer was uniform before the addition of calcium, Fig. 5 *a*. Lipid domains appeared immediately upon adding calcium to the 30 mol % PG bilayer (Fig. 5 *b*). FRAP experiments were performed to determine whether the lipids in the PG-enriched dark domains were mobile, and recovery was observed on a timescale consistent with fluid-fluid separation.

Enhanced clustering of α-synuclein was observed on a PG-containing bilayer pretreated with calcium (Fig. 6). For comparison, a bilayer-protein system in the absence of calcium is shown in Fig. 6, *a* and *c* (these are the same images as in Fig. 1, *b* and *f*, 30 mol % PG bilayer after the addition of 2.6 μM α-synuclein). When 2.6 μM α-synuclein was added to a 30 mol % PG bilayer that was preexposed to calcium (1 mM) (Fig. 6 *d*), the protein preferentially bound to the PG-enriched domains (compare linescans in Fig. 6, *e* and *f*). Calcium-induced protein clusters remained even after the bulk solution was exchanged with EDTA-containing buffer. More dramatic results were obtained with bilayers containing 40 and 50 mol % PG. Clustering could be observed at 30, 40, and 50 mol % PG when the protein concentration was 10-fold lower (0.26 μM). At 50 mol % PG, where the most dramatic reorganization was observed, the calcium concentration could be dropped as low as 25 μM to induce protein clustering at 0.26 μM α-synuclein.

For four cases the amount of protein bound in the clusters was compared with similar areas of protein bound in the absence of calcium. In the case of 2.6 μM added to 30 mol % PG and 0.26 μM added to 50 mol % PG, protein clusters were not observed in the absence of calcium. In both cases, the intensity in the clusters was significantly greater—6(±2)-fold and 6(±1)-fold respectively—than the approximately uniformly adsorbed protein in the absence of calcium (Figs. 1 *f* and 3 *c*).

When 2.6 μM α-synuclein was added to 40 mol % PG or 50 mol % PG, protein clusters were observed in both the absence and presence of calcium (Fig. 1, *g* and *h*, and data not shown). The clusters were roughly the same area and density regardless of whether protein or calcium was added first. In the case of calcium added before protein, the clusters were so intense that the CCD camera maxed out; thus, we can only report lower limits. There was at least threefold (40 mol % PG bilayer) and at least twofold (50 mol % PG bilayer) more protein bound in the clusters of membranes pretreated with calcium. The similar end result, regardless of order of addition, suggests that equilibrium was reached. The observation that more protein bound to bilayers pretreated with calcium is explained by the fact that when calcium was added after protein, the excess protein was rinsed away before the calcium was added, limiting the amount of protein that could bind. In the absence of calcium, the PG-rich domains were ~30% (40 mol % PG bilayer) and ~50% (50 mol % PG bilayer) depleted of NBD-PC. In presence of calcium, the PG-rich domains were ~37% (40 mol % PG bilayer) and ~55% (50 mol % PG bilayer) depleted of NBD-PC.

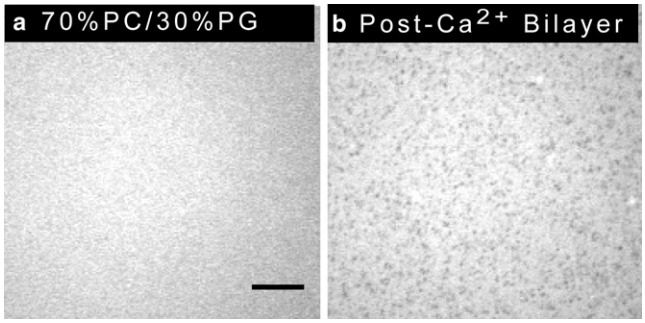

FIGURE 5 Calcium causes phase separation in a PC/PG supported lipid bilayer. Epifluorescence images of a 69.75 mol % PC/ 30 mol % PG/0.25 mol % NBD-PC bilayer are shown. Bilayer (*a*) in the absence of calcium, and (*b*) after the addition of 1 mM calcium. A 100×, 1.3 NA objective was used to acquire the images. The scale bar represents 10 μm.

DISCUSSION

In this study we monitored the adsorption of α-synuclein on supported lipid bilayers via fluorescence microscopy. An important advantage of this approach is that it enables characterization of the lipid and protein distributions on the bilayer surface. In contrast, this spatial information is inaccessible to classic averaging techniques used to monitor protein-lipid interactions in solution. A fluorescence microscopy setup similar to the one described here was recently used to analyze interactions of α-synuclein with discrete domains on giant unilamellar vesicles (28).

α-Synuclein exhibits enhanced affinity for phospholipid bilayers enriched with PG

We found that α-synuclein binds with high affinity to phospholipid membranes under all conditions detailed in this article. Upon adsorbing to the membrane, the protein undergoes a decrease in entropy that must be compensated for by favorable protein-lipid interactions, including hydrophobic and electrostatic interactions. In the experiments described here, α-synuclein binding occurred at very low ionic strength. If the monovalent ion concentration was increased to 750 mM, the binding of the protein to membranes consisting of 50% PG was reduced by ~3-fold (data not shown). However, if the bilayer was exposed to 750 mM solution *after* α-synuclein adsorption, then <10% of the protein desorbed. This hysteresis in the binding-unbinding transition indicates that both hydrophobic and electrostatic interactions play an important role in stabilizing the membrane-bound state of α-synuclein (29).

The affinity of α-synuclein for the bilayer increased dramatically with increasing PG content. This enhanced affinity may reflect an increase in the α-helical content of the protein as it binds membranes with higher amounts of anionic phospholipid. The amphipathic helical form of α-synuclein allows for an optimal distribution of charges, with cationic residues at the protein-lipid interface where they can interact with the anionic headgroups, and with anionic residues exposed to the solvent away from negatively charged phospholipids (23,25,26). Accordingly, an increase in the α-helical content of α-synuclein is predicted to promote interactions between the protein and membrane by favoring electrostatic attraction and disfavoring electrostatic repulsion. In support of this model, data from far-ultraviolet circular dichroism analyses suggest that α-synuclein adopts a more extensive α-helical conformation with enhanced thermal stability upon binding to vesicles with increased PG content (44). Our findings are consistent with previous data showing that α-synuclein preferentially binds vesicles enriched with anionic phospholipids (22,28,45).

α-Synuclein induces PG clustering

The association of α-synuclein with bilayers containing 40 or 50% PG led to a pronounced clustering of the anionic phospholipid. These findings are consistent with NMR data

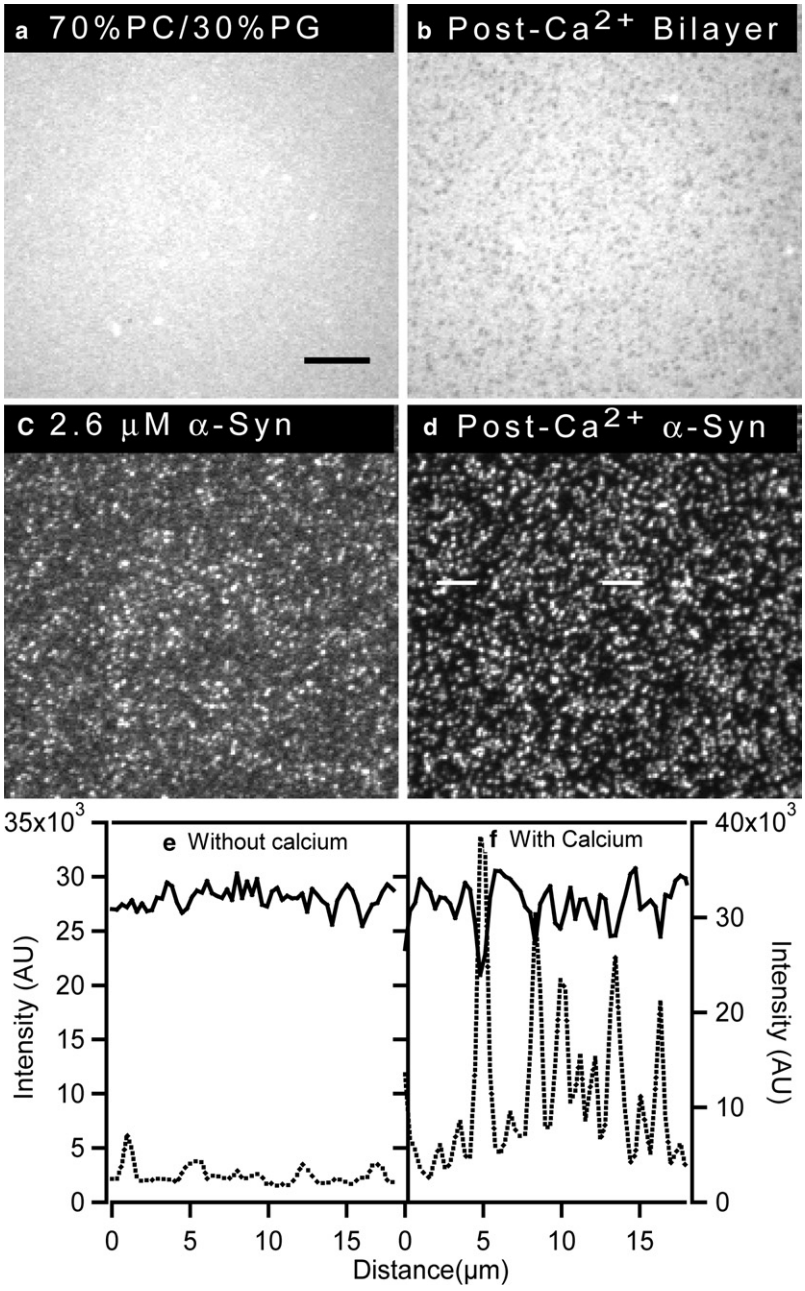

FIGURE 6 α-Synuclein exhibits more pronounced clustering on a supported bilayer in the presence of Ca^{2+} (addition of Ca^{2+} before the protein). Epifluorescence images of 69.75 mol % PC/ 30 mol % PG/0.25 mol % NBD-PC bilayers and α-synuclein are shown. (*a* and *c*) Bilayer (*a*) and protein (*c*) after addition of 2.6 μM α-synuclein in the absence of calcium. (*b* and *d*) Bilayer (*b*) and protein (*d*) after addition of first 1 mM calcium and then 2.6 μM α-synuclein. (*e* and *f*) Corresponding linescans of bilayer (*solid line*, left, *y* axis) and protein (*dotted line*, right, *y* axis) images. Excess α-synuclein was removed before imaging. The protein linescan for α-synuclein in the presence of calcium was taken from the region between the white lines indicated on *d*. A 100×, 1.3 NA objective was used to acquire the images. The scale bar represents 10 μm.

suggesting that α-synuclein induces the formation of PG-rich domains upon binding to PC-PG vesicles (40). One driving force for this lipid reorganization may be the neutralization of charges on helical α-synuclein by PG. The segment of the protein spanning residues 1–95 has 12 cationic residues (all lysines) and nine anionic residues (eight glutamates and one aspartate). When α-synuclein adopts a helical conformation, the lysine residues are predominantly found at the interfacial region, whereas the anionic residues are exclusively located on the solvent-exposed face (23,25,26). The average charge density of 12 lysine residues aligned on the same face of an amphipathic helix with a length of ~15 nm and a width of 1 nm is ~0.8/nm^2. Assuming that all of the phospholipids have a cross-sectional surface area of 65 Å^2 and they are hexagonally packed, the average charge density of a PC-PG bilayer with 30, 40, or 50 mol % PG is ~0.38/nm^2, ~0.50/nm^2, or ~0.63/nm^2, respectively. To meet the conditions of charge neutrality, the lipids must reorganize to create zones of high local PG concentration in response to protein adsorption.

Another driving force for PG clustering may be the energetic benefit associated with PC-PG demixing. In the absence of lipid-lipid interactions, entropy drives the mixing of lipids. Because PC and PG have different physicochemical properties (46,47), PG-PG and PC-PC interactions are likely to be more favorable than PC-PG interactions. Although chain-matched PC and PG have approximately identical T_m values, PC-PG interactions may nevertheless be less favorable than PC-PC or PG-PG interactions. Despite the decrease in entropy, the free energy may be reduced upon PC-PG demixing. Although PC-PG demixing is normally suppressed at pH 7.4 by electrostatic repulsion between the PG lipids, presumably this inhibitory effect is relieved by neutralization of the negative charge on PG after α-synuclein binding.

Because we failed to detect PG clustering after α-synuclein adsorption to the 30 mol % PG bilayer, we infer that the protein only induces lipid reorganization in membranes where the anionic phospholipid content is above some threshold value ($30 < x \leq 40$ mol % PG in PC; Fig. 7). The lower the level of PG in the membrane, the more reorganization is required for charge neutralization. Consequently, there may be a threshold where the entropic cost of reorganization is too great. Another possibility is that the threshold for immiscibility of PG in PC has not been crossed. In a standard model of mixing (e.g., oil in water), molecule A has some solubility in molecule B, and demixing does not occur until a threshold value is reached.

The absence of lipid reorganization in 30 mol % PG bilayers implies that α-synuclein adopts a less α-helical structure upon binding to membranes with lower amounts of anionic phospholipid (Fig. 7). In the absence of PG clustering, the charge density associated with the aligned lysine residues of helical α-synuclein will not be neutralized, and therefore the extended amphipathic helix will be unstable. Under these conditions, α-synuclein may bind to the bilayer as a largely unfolded conformer with relatively little α-helical structure. This mode of binding would involve primarily hydrophobic interactions between the protein and lipids. Anionic lipid clustering would not be necessary to achieve charge neutrality in this case because the lysine residues would be distributed throughout the unfolded α-synuclein structure rather than being aligned on the same face of a helix, and therefore the positive charge density associated with the lysines would be substantially diminished. Normally, electrostatic repulsion between negatively charged residues and anionic phospholipids should favor conversion of membrane-bound, unfolded α-synuclein to the helical form, with anionic residues placed on the solvent face away from the membrane. However, this repulsive effect is expected to play a lesser role in driving α-synuclein helix formation in bilayers containing lower amounts of anionic lipid.

α-Synuclein forms clusters on membranes enriched with anionic phospholipid

The binding of α-synuclein to PC-PG bilayers resulted in the formation of protein clusters that coincide with PG rich-domains. The fluorescence intensity of the α-synuclein clusters increased relative to background with increasing PG content and protein concentration. These findings imply that favorable protein-protein contacts occur in discrete regions of the bilayer enriched with anionic phospholipid (Fig. 7). This behavior may be attributed in part to the migration of PG-associated α-synuclein molecules into PG-rich clusters during phospholipid demixing (47,48). Another explanation may be that the protein adopts a more extensive α-helical structure upon binding to membranes with higher amounts of PG (see above) (44). Although the formation of an amphipathic α-helix is predicted to enhance the affinity of α-synuclein for the membrane, it may also be disfavored by the exposure of several hydrophobic residues on the polar face of the helix. Assuming an α11/3 helical structure, these residues include Met^5, Val^{16}, Leu^{38}, Val^{49}, Val^{71}, Val^{82}, and Phe^{94} (26,29). Two of these residues, Val^{71} and Val^{82}, are part of a hydrophobic, 12-residue segment that is essential for α-synuclein self-assembly in solution (49). Of importance, the exposed hydrophobic residues may be sequestered from the solvent upon binding of additional α-synuclein molecules (originating from elsewhere on the bilayer or from the bulk solvent) to the membrane-bound, helical protein (Fig. 7). The burial of these residues, coupled with the energetically favorable release of solvating water molecules, may be a major driving force for α-synuclein cluster formation. This model is consistent with the results of a computational study showing that the dimerization of helical α-synuclein on a bilayer surface is energetically favorable (29). In addition, α-synuclein forms helical oligomers in solutions containing fluorinated alcohols, which have low dielectric constants that mimic the nonpolar environment at the surface of a phospholipid membrane (J.-C. Rochet, unpublished data) (50).

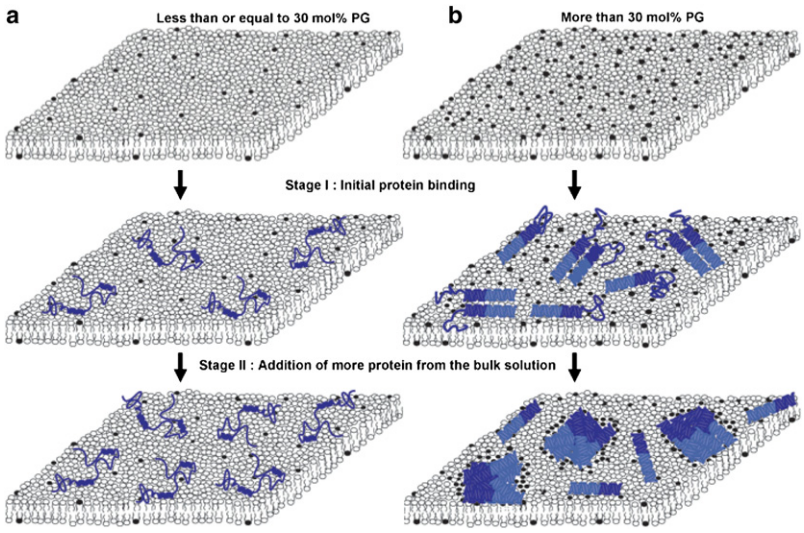

FIGURE 7 Protein binding model on a bilayer surface with high and low amounts of anionic PG lipids. (*a*) On a bilayer with ≤30 mol % PG, α-synuclein is largely unstructured at both stages I and II. (*b*) On a bilayer with >30 mol % PG, α-synuclein is predominantly α-helical. The NAC region is represented by the dark-blue helix and the C-terminus is represented by the blue coil. At stage II the PG lipids (*black lipids*) are clustered. To simplify the illustration, the C-terminus is not shown in stage II.

The increase in α-synuclein cluster formation with increasing PG content may also reflect a decrease in repulsive interactions between neighboring protein molecules. The segment spanning residues 104–140 in the C-terminal domain of α-synuclein contains 14 anionic residues (four aspartates and 10 glutamates). An isolated peptide comprising residues 120–140 has been shown to bind lipid vesicles, with a greater affinity for membranes containing PC alone than membranes enriched with anionic phospholipids (40). Therefore, despite its anionic character, the C-terminal domain may associate with PC-rich membranes through reduced anionic-anionic repulsion, generic van der Waals interactions, and/or attractive electrostatic interactions with the cationic methylamine group of the PC headgroup. When bound to the membrane, the C-terminal tails of adjacent molecules may interfere with α-synuclein oligomerization via electrostatic repulsion. As the PG content is increased, the C-terminal domain may interact less tightly with the membrane, resulting in decreased interference of the protein-protein contacts required for α-synuclein self-assembly on the bilayer surface.

Clustering increases with divalent ion concentration and is independent of addition order

The formation of α-synuclein clusters on PC-PG bilayers was stimulated by divalent metal ions. For example, clusters were observed on a 30 mol % PG bilayer treated with 2.6 μM α-synuclein or on a 50 mol % PG bilayer treated with 0.26 μM α-synuclein in the presence, but not the absence, of 1 mM Ca^{2+}. Previous findings suggest that Ca^{2+} binds to the tail region of α-synuclein, thereby increasing the rigidity of this domain and triggering its interaction with the bilayer (41,51,52). However, two observations suggest that Ca^{2+}-α-synuclein interactions are not a primary driving force for the metal ion-induced clustering described here. First, cluster formation is stimulated to equal extents by Ca^{2+} and Mg^{2+} (data not shown), whereas only Ca^{2+} (not Mg^{2+}) promotes the interaction of the C-terminal domain with phospholipid membranes (41). Second, similar clustering patterns are observed regardless of whether Ca^{2+} or α-synuclein is added first to the bilayer, and the α-synuclein and PG clusters exhibit extensive overlap. These results suggest that divalent metal ions induce the formation of α-synuclein clusters by triggering PC-PG demixing, presumably via a mechanism involving partial neutralization of the anionic charge on PG. Consistent with this model, we and others (42,43) have shown that Ca^{2+} induces lipid reorganization in bilayers consisting of mixtures of anionic and zwitterionic phospholipids. Of importance, our results indicate that the binding of α-synuclein to PG-rich clusters is enhanced when the bilayer is treated with Ca^{2+} before rather than after the addition of protein. This increased binding may be due to stabilization of the high-affinity helical form of α-synuclein by PG-rich clusters generated in the presence of Ca^{2+}.

Physiological implications

The results of our study indicate that cluster formation by membrane-bound α-synuclein is stimulated by increased levels of anionic phospholipid, α-synuclein, and Ca^{2+}. We hypothesize that upregulation of each of these parameters may stimulate α-synuclein clustering in the brain during aging and in age-related neurodegenerative diseases such as PD. In support of this idea, it has been observed that the brains of aged rats have elevated levels of phosphatidic acid (53), and the ratio of anionic to zwitterionic phospholipids increases in the brains of PD patients (54). In addition, α-synuclein levels are upregulated in the postmortem brains of elderly individuals and synucleinopathy patients (17,55–59). Disturbances of neuronal calcium homeostasis resulting in Ca^{2+} ''overload'' are associated with aging and neurodegeneration (60,61). Of importance, enhanced α-synuclein cluster

formation may contribute to the pathogenesis of age-related neurologic disorders via diverse mechanisms. For example, the sequestration of α-synuclein in clusters may disrupt interactions between the protein and the dopamine transporter (20). In turn, the resulting upregulation of dopamine transporter activity may play a role in dopaminergic cell death. The formation of membrane-bound α-synuclein clusters may also promote conversion of the protein to potentially toxic, high-molecular-weight assemblies (30), especially under conditions that trigger dissociation of the protein from the membrane and/or β-sheet formation (e.g., oxidative stress or elevated Ca^{2+} concentrations) (41,62).

CONCLUSIONS

The results and discussion presented here lead to the following conclusions: 1), the increased affinity of α-synuclein for membranes with higher amounts of anionic phospholipid may reflect an increase in the α-helical content of the protein; 2), the lipid demixing observed upon α-synuclein membrane binding may be driven by the need to neutralize the charges on helical α-synuclein and/or relieve unfavorable PC-PG interactions; 3), α-synuclein clustering may be driven by the requirement to bury hydrophobic residues that are exposed when the protein adopts an α-helical conformation; and 4), divalent metal ions may stimulate cluster formation by promoting PC-PG demixing. Because the formation of membrane-bound α-synuclein assemblies may play a role in neurotoxicity, strategies to interfere with clustering may prove beneficial for the treatment of PD and other synucleinopathy disorders.

We thank Jagadish Kumar Hindupur and John Hulleman for assistance with α-synuclein expression, purification, and labeling.

This work was supported in part by National Institutes of Health grant R01 NS049221 and the Showalter Trust.

REFERENCES

1. Pollanen, M. S., D. W. Dickson, and C. Bergeron. 1993. Pathology and biology of the Lewy body. *J. Neuropathol. Exp. Neurol.* 52:183–191.
2. Forno, L. S. 1996. Neuropathology of Parkinson's disease. *J. Neuropathol. Exp. Neurol.* 55:259–272.
3. Takahashi, H., and K. Wakabayashi. 2001. The cellular pathology of Parkinson's disease. *Neuropathology.* 21:315–322.
4. Spillantini, M. G., M. L. Schmidt, V. M. -Y. Lee, J. Q. Trojanowski, R. Jakes, et al. 1997. α-Synuclein in Lewy bodies. *Nature.* 388:839–840.
5. Wakabayashi, K., K. Matsumoto, K. Takayama, M. Yoshimoto, and H. Takahashi. 1997. NACP, a presynaptic protein, immunoreactivity in Lewy bodies in Parkinson's disease. *Neurosci. Lett.* 239:45–48.
6. Baba, M., S. Nakajo, P. -H. Tu, T. Tomita, K. Nakaya, et al. 1998. Aggregation of α-synuclein in Lewy bodies of sporadic Parkinson's disease and dementia with Lewy bodies. *Am. J. Pathol.* 152: 879–884.
7. Spillantini, M. G., R. A. Crowther, R. Jakes, M. Hasegawa, and M. Goedert. 1998. α-Synuclein in filamentous inclusions of Lewy bodies from Parkinson's disease and dementia with Lewy bodies. *Proc. Natl. Acad. Sci. USA.* 95:6469–6473.
8. Polymeropoulos, M. H., C. Lavedan, E. Leroy, S. E. Ide, A. Dehejia, et al. 1997. Mutation in the α-synuclein gene identified in families with Parkinson's disease. *Science.* 276:2045–2047.
9. Kruger, R., W. Kuhn, T. Muller, D. Woitalla, M. Graeber, et al. 1998. Ala30Pro mutation in the gene encoding α-synuclein in Parkinson's disease. *Nat. Genet.* 18:106–108.
10. Zarranz, J. J., J. Alegre, J. C. Gomez-Esteban, E. Lezcano, R. Ros, et al. 2004. The new mutation, E46K, of α-synuclein causes Parkinson and Lewy body dementia. *Ann. Neurol.* 55:164–173.
11. Narhi, L., S. J. Wood, S. Steavenson, Y. Jiang, G. M. Wu, et al. 1999. Both familial Parkinson's disease mutations accelerate α-synuclein aggregation. *J. Biol. Chem.* 274:9843–9846.
12. Conway, K. A., S. -J. Lee, J. -C. Rochet, T. T. Ding, R. E. Williamson, et al. 2000. Acceleration of oligomerization, not fibrillization, is a shared property of both α-synuclein mutations linked to early-onset Parkinson's disease: implications for pathogenesis and therapy. *Proc. Natl. Acad. Sci. USA.* 97:571–576.
13. Li, J., V. N. Uversky, and A. L. Fink. 2001. Effect of familial Parkinson's disease point mutations A30P and A53T on the structural properties, aggregation, and fibrillation of human α-synuclein. *Biochemistry.* 40:11604–11613.
14. Fredenburg, R. A., C. Rospigliosi, R. K. Meray, J. C. Kessler, H. A. Lashuel, et al. 2007. The impact of the E46K mutation on the properties of α-synuclein in its monomeric and oligomeric states. *Biochemistry.* 46:7107–7118.
15. Greenbaum, E. A., C. L. Graves, A. J. Mishizen-Eberz, M. A. Lupoli, D. R. Lynch, et al. 2005. The E46K mutation in α-synuclein increases amyloid fibril formation. *J. Biol. Chem.* 280:7800–7807.
16. Choi, W., S. Zibaee, R. Jakes, L. C. Serpell, B. Davletov, et al. 2004. Mutation E46K increases phospholipid binding and assembly into filaments of human α-synuclein. *FEBS Lett.* 576:363–368.
17. Dev, K. K., K. Hofele, S. Barbieri, V. L. Buchman, and H. van der Putten. 2003. Part II: α-Synuclein and its molecular pathophysiological role in neurodegenerative disease. *Neuropharmacology.* 45:14–44.
18. Murphy, D. D., S. M. Rueter, J. Q. Trojanowski, and V. M. Y. Lee. 2000. Synucleins are developmentally expressed, and α-synuclein regulates the size of the presynaptic vesicular pool in primary hippocampal neurons. *J. Neurosci.* 20:3214–3220.
19. Cabin, D. E., K. Shimazu, D. Murphy, N. B. Cole, W. Gottschalk, et al. 2002. Synaptic vesicle depletion correlates with attenuated synaptic responses to prolonged repetitive stimulation in mice lacking α-synuclein. *J. Neurosci.* 22:8797–8807.
20. Sidhu, A., C. Wersinger, and P. Vernier. 2004. α-Synuclein regulation of the dopaminergic transporter: a possible role in the pathogenesis of Parkinson's disease. *FEBS Lett.* 565:1–5.
21. Weinreb, P. H., W. G. Zhen, A. W. Poon, K. A. Conway, and P. T. Lansbury. 1996. NACP, a protein implicated in Alzheimer's disease and learning, is natively unfolded. *Biochemistry.* 35:13709–13715.
22. Davidson, W. S., A. Jonas, D. F. Clayton, and J. M. George. 1998. Stabilization of α-synuclein secondary structure upon binding to synthetic membranes. *J. Biol. Chem.* 273:9443–9449.
23. Jao, C. C., A. Der-Sarkissian, J. Chen, and R. Langen. 2004. Structure of membrane-bound α-synuclein studied by site-directed spin labeling. *Proc. Natl. Acad. Sci. USA.* 101:8331–8336.
24. Ramakrishnan, M., P. H. Jensen, and D. Marsh. 2003. α-Synuclein association with phosphatidylglycerol probed by lipid spin labels. *Biochemistry.* 42:12919–12926.
25. Bussell, R., T. F. Ramlall, and D. Eliezer. 2005. Helix periodicity, topology, and dynamics of membrane-associated α-synuclein. *Protein Sci.* 14:862–872.
26. Bussell, R., Jr., and D. Eliezer. 2003. A structural and functional role for 11-mer repeats in α-synuclein and other exchangeable lipid binding proteins. *J. Mol. Biol.* 329:763–778.
27. Chandra, S., X. C. Chen, J. Rizo, R. Jahn, and T. C. Sudhof. 2003. A broken α-helix in folded α-synuclein. *J. Biol. Chem.* 278: 15313–15318.

28. Stockl, M., P. Fischer, E. Wanker, and A. Herrmann. 2008. α-Synuclein selectively binds to anionic phospholipids embedded in liquid-disordered domains. *J. Mol. Biol.* 375:1394–1404.
29. Mihajlovic, M., and T. Lazaridis. 2008. Membrane-bound structure and energetics of α-synuclein. *Proteins.* 70:761–778.
30. Lee, H. -J., C. Choi, and S. -J. Lee. 2002. Membrane-bound α-synuclein has a high aggregation propensity and the ability to seed the aggregation of the cytosolic form. *J. Biol. Chem.* 277:671–678.
31. Necula, M., C. N. Chirita, and J. Kuret. 2003. Rapid anionic micelle-mediated α-synuclein fibrillization in vitro. *J. Biol. Chem.* 278:46674–46680.
32. Beyer, K. 2007. Mechanistic aspects of Parkinson's disease: α-synuclein and the biomembrane. *Cell Biochem. Biophys.* 47:285–299.
33. Narayanan, V., and S. Scarlata. 2001. Membrane binding and self-association of α-synucleins. *Biochemistry.* 40:9927–9934.
34. Zhu, M., and A. L. Fink. 2003. Lipid binding inhibits α-synuclein fibril formation. *J. Biol. Chem.* 278:16873–16877.
35. Sackmann, E. 1996. Supported membranes: scientific and practical applications. *Science.* 271:43–48.
36. Seu, K. J., A. P. Pandey, F. Haque, E. A. Proctor, A. E. Ribbe, et al. 2007. Effect of surface treatment on diffusion and domain formation in supported lipid bilayers. *Biophys. J.* 92:2445–2450.
37. Findlay, E. J., and P. G. Barton. 1978. Phase behavior of synthetic phosphatidylglycerols and binary-mixtures with phosphatidylcholines in presence and absence of calcium-ions. *Biochemistry.* 17:2400–2405.
38. Garidel, P., C. Johann, L. Mennicke, and A. Blume. 1997. The mixing behavior of pseudobinary phosphatidylcholine phosphatidylglycerol mixtures as a function of pH and chain length. *Eur. Biophys. J.* 26:447–459.
39. Seu, K., L. R. Cambrea, R. M. Everly, and J. S. Hovis. 2006. Influence of lipid chemistry on membrane fluidity: tail and headgroup interactions. *Biophys. J.* 91:3727–3735.
40. Madine, J., A. J. Doig, and D. A. Middleton. 2006. A study of the regional effects of α-synuclein on the organization and stability of phospholipid bilayers. *Biochemistry.* 45:5783–5792.
41. Tamamizu-Kato, S., M. G. Kosaraju, H. Kato, V. Raussens, J. M. Ruysschaert, et al. 2006. Calcium-triggered membrane interaction of the α-synuclein acidic tail. *Biochemistry.* 45:10947–10956.
42. Evert, L. L., D. Leckband, and J. N. Israelachvili. 1994. Structure and dynamics of ion-induced domains in free and supported monolayers and bilayers. *Langmuir.* 10:303–315.
43. Lamberson, E. R., L. R. Cambrea, and J. S. Hovis. 2007. Controlling the charge and organization of anionic lipid bilayers: effect of monovalent and divalent ions. *J. Phys. Chem. B.* 111:13664–13667.
44. Zakharov, S. D., J. D. Hulleman, E. A. Dutseva, Y. N. Antonenko, J. C. Rochet, et al. 2007. Helical α-synuclein forms highly conductive ion channels. *Biochemistry.* 46:14369–14379.
45. Jo, E., J. McLaurin, C. M. Yip, P. St. George-Hyslop, and P. E. Fraser. 2000. α-Synuclein membrane interactions and lipid specificity. *J. Biol. Chem.* 275:34328–34334.
46. Hinderliter, A., P. F. Almeida, C. E. Creutz, and R. L. Biltonen. 2001. Domain formation in a fluid mixed lipid bilayer modulated through binding of the C2 protein motif. *Biochemistry.* 40:4181–4191.
47. Mbamala, E. C., A. Ben-Shaul, and S. May. 2005. Domain formation induced by the adsorption of charged proteins on mixed lipid membranes. *Biophys. J.* 88:1702–1714.
48. May, S., D. Harries, and A. Ben-Shaul. 2000. Lipid demixing and protein-protein interactions in the adsorption of charged proteins on mixed membranes. *Biophys. J.* 79:1747–1760.
49. Giasson, B. I., I. V. J. Murray, J. Q. Trojanowski, and V. M. Y. Lee. 2001. A hydrophobic stretch of 12 amino acid residues in the middle of α-synuclein is essential for filament assembly. *J. Biol. Chem.* 276:2380–2386.
50. Munishkina, L. A., C. Phelan, V. N. Uversky, and A. L. Fink. 2003. Conformational behavior and aggregation of α-synuclein in organic solvents: modeling the effects of membranes. *Biochemistry.* 42:2720–2730.
51. Nielsen, M. S., H. Vorum, E. Lindersson, and P. H. Jensen. 2001. Ca^{2+} binding to α-synuclein regulates ligand binding and oligomerization. *J. Biol. Chem.* 276:22680–22684.
52. de Laureto, P. P., L. Tosatto, E. Frare, O. Marin, V. N. Uversky, et al. 2006. Conformational properties of the SDS-bound state of α-synuclein probed by limited proteolysis: unexpected rigidity of the acidic C-terminal tail. *Biochemistry.* 45:11523–11531.
53. Giusto, N. M., G. A. Salvador, P. I. Castagnet, S. J. Pasquare, and M. G. Ilincheta de Boschero. 2002. Age-associated changes in central nervous system glycerolipid composition and metabolism. *Neurochem. Res.* 27:1513–1523.
54. Riekkinen, P., U. K. Rinne, T. T. Pelliniemi, and V. Sonninen. 1975. Interaction between dopamine and phospholipids. Studies of the substantia nigra in Parkinson disease patients. *Arch. Neurol.* 32:25–27.
55. Dawson, T. M., and V. L. Dawson. 2003. Molecular pathways of neurodegeneration in Parkinson's disease. *Science.* 302:819–822.
56. Singleton, A. B., M. Farrer, J. Johnson, A. Singleton, S. Hague, et al. 2003. α-Synuclein locus triplication causes Parkinson's disease. *Science.* 302:841.
57. Li, W. X., C. Lesuisse, Y. Q. Xu, J. C. Troncoso, D. L. Price, et al. 2004. Stabilization of α-synuclein protein with aging and familial Parkinson's disease-linked A53T mutation. *J. Neurosci.* 24:7400–7409.
58. Chu, Y., and J. H. Kordower. 2007. Age-associated increases of α-synuclein in monkeys and humans are associated with nigrostriatal dopamine depletion: is this the target for Parkinson's disease? *Neurobiol. Dis.* 25:134–149.
59. Kovacs, G. G., I. J. Milenkovic, M. Preusser, and H. Budka. 2008. Nigral burden of α-synuclein correlates with striatal dopamine deficit. *Mov. Disord.* 23:1608–1612.
60. Toescu, E. C., and A. Verkhratsky. 2000. Parameters of calcium homeostasis in normal neuronal ageing. *J. Anat.* 197:563–569.
61. Mattson, M. P. 2007. Calcium and neurodegeneration. *Aging Cell.* 6:337–350.
62. Hodara, R., E. H. Norris, B. I. Giasson, A. J. Mishizen-Eberz, D. R. Lynch, et al. 2004. Functional consequences of α-synuclein tyrosine nitration: diminished binding to lipid vesicles and increased fibril formation. *J. Biol. Chem.* 279:47746–47753.